

Effect of topology on the critical charge in graphene

Baishali Chakraborty^{1,*}, Kumar S. Gupta^{1,†} and Siddhartha Sen^{2‡}

¹*Theory Division, Saha Institute of Nuclear Physics,
1/AF Bidhannagar, Calcutta 700064, India*

²*Trinity College, Dublin, Ireland*

(Dated: March 24, 2021)

We show that the critical charge for the Dirac excitations in gapless graphene depends on the spatial topology of the sample. In particular, for graphene cones, the effective value of the critical charge can tend towards zero for a suitable angle of the conical sample. We discuss the nature of the scattering phase shifts, quasi-bound state energies and local density of states for a gapless graphene cone and determine the dependence of these physical quantities on the sample topology.

INTRODUCTION

The fabrication of monolayer graphene [1–3] provides an opportunity to study the effect of sample topology on its electronic properties [4–9]. The low energy excitations of the gapless graphene are described by a two dimensional massless Dirac equation [10–14]. These excitations are negatively charged and behave like electrons with the Fermi velocity $v_F \approx 10^6 m/s$. In graphene, even a small external charge impurity $Ze \sim 1$ can produce strong nonperturbative effects, since the effective Coulomb interaction strength $\alpha = \frac{Ze^2}{\hbar\kappa v_F} \sim 1$, where the dielectric constant $\kappa \sim 5$. Thus, graphene provides an ideal system to analyze the combined effects of topology and strong electric fields on its electronic properties.

The idea of a critical charge plays an interesting role in this context [15–19]. It is well known that massless Dirac fermions can tunnel through large external potentials, thereby avoiding trapping or formation of bound states. This phenomenon, known as Klein tunneling [20–24], is possible in graphene due to the chiral nature of the Dirac excitations [18, 20]. However, when the effective strength of the external charge exceeds a certain critical value α_c , the low energy excitations can form quasi-bound states [15–19]. For such states the wavefunctions oscillate rapidly near the position of the charge impurity, analogous to *zitterbewegung* in strong field QED [24, 25]. For planar graphene, the critical charge $\alpha_c = \frac{1}{2}$. The existence of such quasi-bound states and their effect on transport properties and local density of states (LDOS) in planar graphene have attracted considerable attention [15–18].

In this paper we explore how a nontrivial topology of the sample may affect the critical charge and the corresponding strong field QED effects in graphene. We address this issue for graphene cones, which are obtained by introducing local defects in the hexagonal lattice structure, for example, in the form of a pentagonal ring [4, 5]. The conical topology manifests itself in the form of nontrivial holonomies for the pseudoparticle wavefunctions. Such holonomies can be modelled through the introduction of a magnetic flux tube. Thus an electric charge localized at the apex of the cone can be equivalently described by a suitable combination of electric charge and magnetic flux tube. We show that the critical charge α_c depends on the angle of the graphene cone. For certain angle of the graphene cone, the topological effects lead to the identification of the two Fermi points [4, 5]. This leads to the surprising conclusion that for a certain value of the angle of the cone, the critical charge is zero. We discuss the effect of the conical topology on the scattering phase shifts, quasi-bound state energies and local density of states (LDOS) in graphene.

This paper is organized as follows. In the next Section we set up the Dirac equation for gapless graphene cone with a point charge at the apex. This is followed by the analysis of the corresponding spectrum, where we obtain the scattering phase shifts, quasi-bound state energies and local density of states (LDOS) and show how these physical quantities depend explicitly on the sample topology. We also briefly comment on the RG flow of the strength of the charge impurity. We end this paper with some discussion and outlook.

DIRAC EQUATION FOR A GRAPHENE CONE WITH A COULOMB CHARGE

In this section we set up the Dirac equation for a graphene cone with a coulomb charge at the apex of the cone. The low energy properties of the quasiparticle states near the Dirac points in graphene can be described by the four component Dirac wave function [10–12] given by

$$\Psi = \begin{pmatrix} \Psi_A \\ \Psi_B \end{pmatrix}, \quad \text{where } \Psi_A = \begin{pmatrix} \Psi_{A+} \\ \Psi_{A-} \end{pmatrix} \quad \text{and} \quad \Psi_B = \begin{pmatrix} \Psi_{B+} \\ \Psi_{B-} \end{pmatrix} \quad (1)$$

The pseudospin indices A and B label the two sublattices of the primitive cell of graphene and the valley indices $+$ and $-$ label the two inequivalent Dirac points \mathbf{K}_+ and \mathbf{K}_- respectively.

Considering low energy excitations about the Dirac point K_+ , Dirac equation for a planar gapless graphene in the presence of a Coulomb charge Ze is given by

$$H\Psi = \left[-i\hbar v_F(\sigma_1\partial_x + \sigma_2\partial_y) + \sigma_0 \left(\frac{-\alpha}{r} \right) \right] \Psi = E\Psi, \quad (2)$$

where r is the radial coordinate in the two dimensional $x-y$ plane. The Pauli matrices $\sigma_{1,2,3}$ and the identity matrix σ_0 act on the pseudospin indices A, B . The Coulomb interaction strength $\alpha = \frac{Ze^2}{\hbar\kappa v_F}$. From now on we set $\hbar = v_F = 1$. In a two dimensional plane, the angular boundary condition for a Dirac spinor as it goes around a closed path is given by

$$\Psi(\mathbf{r}, \theta = 2\pi) = e^{i\pi\sigma_3} \Psi(\mathbf{r}, \theta = 0). \quad (3)$$

A cone is obtained from the two dimensional plane by introducing a topological defect, which modifies the angular boundary condition (3). Following [4], consider a cone, formed by removing the sector AOB (see Fig.1a.) and then identifying the edge OA , labeled by $\theta = 0$ with the edge OB , labeled by $\theta = 2\pi$. The sector AOB subtends an angle $\frac{2\pi}{6}$ at the centre O . Due to this identification the frame $\{\hat{e}_x, \hat{e}_y\}$ becomes discontinuous across the joining line. This problem can be solved by choosing a new set of frames given by

$$\hat{e}_{x'} = \hat{e}_\theta \quad \text{and} \quad \hat{e}_{y'} = -\hat{e}_r, \quad (4)$$

which is rotated with respect to old frame (\hat{e}_x, \hat{e}_y) by an angle $\phi = \theta + \frac{\pi}{2}$ in the counter clockwise direction, see Fig.1b. To keep the form of the Hamiltonian the same, the wave function has to be transformed by $\exp(i\phi\sigma_3/2)$. Similarly, if n sectors are removed from the plane where n can take only discrete values 1, 2, 3, 4, 5, the wave function should be transformed as

$$\Psi(\mathbf{r}, \theta = 2\pi) = -e^{i2\pi(1-\frac{n}{6})\frac{\sigma_3}{2}} \Psi(\mathbf{r}, \theta = 0). \quad (5)$$

Note that an additional negative sign appears in the boundary condition since we take the angular part of the wavefunction to be $e^{ij\theta}$, j being a half integer [4, 5].

When n is odd, an additional phase change is required due to the breaking of the bipartite nature of the hexagonal lattice. It can be seen from the Fig.(2), that the removal of a wedge of opening angle $\frac{2\pi}{6}$ introduces a pentagonal defect. When the cone is formed by removing a single wedge of angle $\frac{2\pi}{6}$, the adjacent points on two sides of the identification line belong to the same sublattice. This feature is valid for all allowed odd $n = 1, 3, 5$ and leads to a system with only one Fermi point. Considering all the factors, the angular boundary condition satisfied for a general value of n is given by [4, 5].

$$\Psi(\mathbf{r}, \theta = 2\pi) = -e^{i2\pi[-\frac{n\tau_2}{4} + (1-\frac{n}{6})\frac{\sigma_3}{2}]} \Psi(\mathbf{r}, \theta = 0). \quad (6)$$

Here τ_2 acts on the valley indices $(+, -)$. Note that for $n = 0$, the angular boundary condition for the planar graphene is recovered. For the allowed even values of $n = 2$ and 4, it can be seen from (6) that the matrix τ_2 plays no role in the angular boundary condition [4, 5]. This is due to the fact that for even n , $e^{i2\pi[-\frac{n\tau_2}{4}]} = \cos(\frac{\pm n\pi}{2}) = e^{i\pi[\frac{\pm n}{2}]}$. For odd n , the two Dirac points are identified and the energy eigenstates of the Dirac equation are obtained by diagonalizing τ_2 which mixes the valley indices in the wavefunction [4, 5]. Since the eigenvalues of τ_2 are ± 1 , for all values of n , we can replace the angular boundary condition (6) by

$$\Psi(\mathbf{r}, \theta = 2\pi) = -e^{i2\pi[\pm\frac{n}{4} + (1-\frac{n}{6})\frac{\sigma_3}{2}]} \Psi(\mathbf{r}, \theta = 0). \quad (7)$$

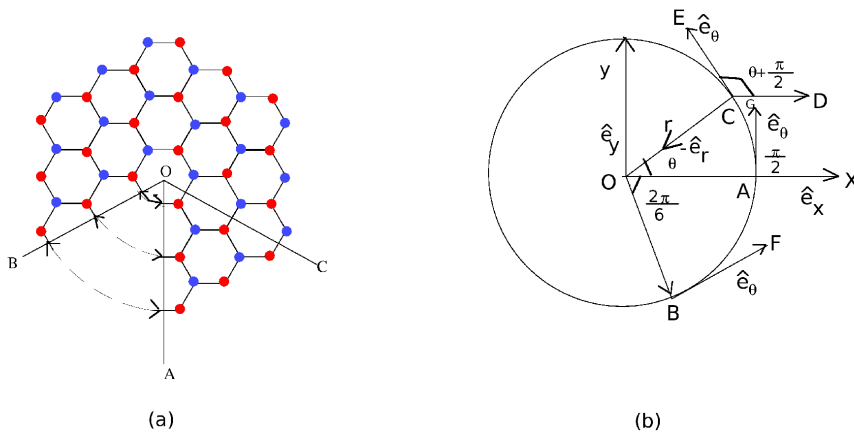


FIG. 1: (a) Formation of a cone from plane graphene sheet by cut and paste procedure and (b) Rotation of the coordinate frame due to its new orientation. In Fig. (a) blue atoms represent sublattice A and red atoms represent sublattice B.

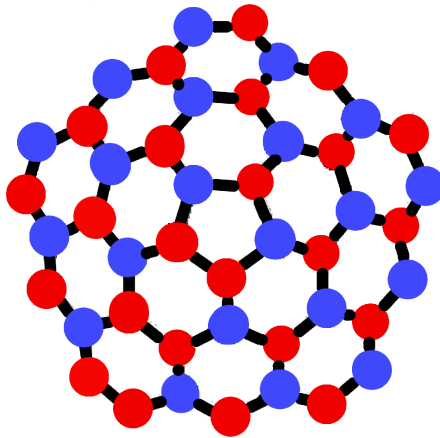


FIG. 2: A Graphene cone formed by removing an angular sector of $\frac{2\pi}{6}$ from the plane sheet.

In subsequent analysis, we shall use the form (7) of the angular boundary condition assuming that for all allowed odd values of n , the matrix τ_2 acting on the valley indices has already been diagonalized.

The effect of the angular boundary condition (7) on the wave function can be equivalently described by introducing a magnetic flux tube passing through the apex of the cone [4]. The presence of a magnetic vector potential modifies the boundary condition on a Dirac spinor as

$$\Psi(\mathbf{r}, \theta = 2\pi) = -e^{ie\oint \vec{A} \cdot d\vec{l}} \Psi(\mathbf{r}, \theta = 0). \quad (8)$$

Taking $d\vec{l}$ as a line element on the circumference of the cone at a distance r from the apex, we have

$$d\vec{l} = \hat{e}_\theta r \left(1 - \frac{n}{6}\right) d\theta. \quad (9)$$

Substituting (9) in (8) and assuming that A_θ is independent of the angle θ , we get

$$\Psi(\mathbf{r}, \theta = 2\pi) = -e^{ie2\pi r \left(1 - \frac{n}{6}\right) A_\theta} \Psi(\mathbf{r}, \theta = 0). \quad (10)$$

TABLE I: The values of critical charge α_c i.e the minimum values of $|\nu|$ for different values of opening angle of the graphene cone i.e for different values of n . The values of angular momentum j for which we get the critical charge are also noted.

value of n	Critical charge (α_c)	Corresponding angular momentum (j)
0	0.5	$\pm\frac{1}{2}$
1	0.3	$\pm\frac{1}{2}$
2	0	$\pm\frac{1}{2}$
3	0.5	$\pm\frac{1}{2}$
4	1.5	$\pm\frac{1}{2}$
5	1.5	$\pm\frac{3}{2}$

Comparing equation (7) and equation (10) we get

$$A_\theta = \frac{1}{er} \left[\pm \frac{\frac{n}{4}}{(1 - \frac{n}{6})} + \frac{\sigma_3}{2} \right]. \quad (11)$$

Thus the entire effect of the conical topology on the wavefunction can be described by introducing the vector potential (10), which replaces the ordinary derivatives by the corresponding covariant derivatives in the Hamiltonian (2). In this effective description, the Hamiltonian for a graphene cone with a Coulomb charge at the apex is given by

$$H = -i(\sigma_1 \partial_{x'} + \sigma_2 \partial_{y'}) - e(\vec{\sigma} \cdot \hat{e}_\theta) A_\theta - \sigma_0 \left(\frac{-\alpha}{r} \right), \quad (12)$$

where the relation between (x', y') and (r, θ) can be obtained from the Equation(4), which gives $\partial_{x'} = \frac{1}{r(1-\frac{n}{6})} \partial_\theta$ and $\partial_{y'} = -\partial_r$ and $\vec{\sigma} \cdot \hat{e}_\theta = \sigma_1$. Thus the Dirac equation (2) can be written as

$$H \begin{pmatrix} \Psi_A \\ \Psi_B \end{pmatrix} = \begin{pmatrix} -\frac{\alpha}{r} & \partial_r - \frac{i}{r(1-\frac{n}{6})} \partial_\theta \pm \frac{\frac{n}{4}}{r(1-\frac{n}{6})} + \frac{1}{2r} \\ -\partial_r - \frac{i}{r(1-\frac{n}{6})} \partial_\theta \pm \frac{\frac{n}{4}}{r(1-\frac{n}{6})} - \frac{1}{2r} & -\frac{\alpha}{r} \end{pmatrix} \begin{pmatrix} \Psi_A \\ \Psi_B \end{pmatrix} = E \begin{pmatrix} \Psi_A \\ \Psi_B \end{pmatrix} \quad (13)$$

We use an ansatz for the wavefunction given by

$$\Psi(r, \theta) = \sum_j \begin{pmatrix} \Psi_A^{(j)}(r) \\ i\Psi_B^{(j)}(r) \end{pmatrix} e^{-iEr} r^{\gamma-\frac{1}{2}} e^{ij\theta}, \quad (14)$$

where the total angular momentum j takes all half integer values. Substituting (14) in (13), we note that the leading short distance behaviour of the wavefunction is given by

$$\Psi_{A,B}^{(j)}(r) \sim r^{\gamma-\frac{1}{2}} \quad \text{where} \quad \gamma = \sqrt{\nu^2 - \alpha^2} \quad \text{and} \quad \nu = \frac{(j \pm \frac{n}{4})}{(1 - \frac{n}{6})}. \quad (15)$$

From (15) it follows that when $|\alpha|$ exceeds $|\nu|$, γ becomes imaginary. As a result, the eigenstates $\Psi_A^{(j)}(r)$ and $\Psi_B^{(j)}(r)$ becomes wildly oscillatory and have no well defined limit as $r \rightarrow 0$, which corresponds to the phenomenon of zitterbewegung in a strong Coulomb electric field [25]. The critical value of the coupling is denoted by α_c and it is given by the minimum allowed value of $|\nu|$. The parameter ν depends on j and the number of sectors n removed from a plane to form the graphene cone. Hence we see that the critical coupling α_c explicitly depends on the angle of the graphene cone. The values of the critical charge for different values of n are given in TABLE I.

From these values of critical charge, a surprising result can be observed for the case of $n = 2$, where α_c is zero. In this case, any external charge will be supercritical. We should also note that when $n = 5$, none of the values of ν in the lowest angular momentum channel $j = \pm\frac{1}{2}$, corresponds to the minimum value of $|\nu|$ or the critical charge. In this case the critical charge of the system is obtained from the angular momentum channel $j = \pm\frac{3}{2}$.

SPECTRUM IN GRAPHENE CONE WITH A SUPERCRITICAL CHARGE

In this Section we derive the scattering and bound state spectra for a gapless graphene cone in the presence of a supercritical Coulomb charge located at the apex of the cone. First consider the case $\nu \neq 0$. Using (13) and (14), the

Dirac equation in each angular momentum channel j can be written as

$$\begin{pmatrix} E + \frac{\alpha}{r} & -\{\partial_r + (\nu + \frac{1}{2})\frac{1}{r}\} \\ \{\partial_r - (\nu - \frac{1}{2})\frac{1}{r}\} & E + \frac{\alpha}{r} \end{pmatrix} \begin{pmatrix} \Psi_A^{(j)}(r) \\ i\Psi_B^{(j)}(r) \end{pmatrix} e^{-iEr} r^{\gamma-\frac{1}{2}} = 0. \quad (16)$$

In terms of the functions $u^{(j)}(r)$ and $v^{(j)}(r)$ defined by $\Psi_A^{(j)}(r) = [v^{(j)}(r) + u^{(j)}(r)]$ and $\Psi_B^{(j)}(r) = [v^{(j)}(r) - u^{(j)}(r)]$, we get

$$r \frac{dv^{(j)}(r)}{dr} + (\gamma + i\alpha)v^{(j)}(r) - \nu u^{(j)}(r) = 0 \quad (17)$$

and

$$r \frac{du^{(j)}(r)}{dr} + (\gamma - i\alpha - 2iEr)u^{(j)}(r) - \nu v^{(j)}(r) = 0. \quad (18)$$

From (17) and (18), we get

$$s \frac{d^2v^{(j)}(s)}{ds^2} + (1 + 2\gamma - s) \frac{dv^{(j)}(s)}{ds} - (\gamma + i\alpha)v^{(j)}(s) = 0, \quad (19)$$

where $s = -2ikr$, with $k = -E$. For the discussion below, for any given value of n and j , we choose α greater than the corresponding value of $|\nu|$. This ensures that the coupling is always in the supercritical region. Define $\gamma = i\lambda$ where $\lambda = \sqrt{\alpha^2 - \nu^2}$. Then the solution of Eq.(19) is given by

$$v^{(j)}(s) = C_1 M(i(\lambda + \alpha), 1 + 2i\lambda, s) + C_2 s^{-2i\lambda} M(i(\alpha - \lambda), 1 - 2i\lambda, s). \quad (20)$$

From (17) and (20) we get

$$u^{(j)}(s) = -iC_1 \mu M(1 + i(\lambda + \alpha), 1 + 2i\lambda, s) - i(C_2/\mu) s^{-2i\lambda} M(1 + i(\alpha - \lambda), 1 - 2i\lambda, s) \quad (21)$$

where $\mu = \sqrt{\frac{\alpha + \lambda}{\alpha - \lambda}}$.

In order to proceed, we use the zigzag edge boundary condition $[u^{(j)}(a_0) - v^{(j)}(a_0)] = 0$, where a_0 is a distance from the apex, of the order of the lattice scale in graphene [16]. This gives

$$C_2 = e^{2i\zeta(k)} \mu e^{\pi\lambda} C_1 \quad \text{where} \quad e^{2i\zeta(k)} = \frac{i(1 + i\mu)}{(1 - i\mu)} e^{2i\lambda \ln(2ka_0)}. \quad (22)$$

From the above, we obtain the scattering matrix S as

$$S = e^{2i\delta_\nu(k)} = \left[\frac{f_{\alpha,\lambda} + e^{2i\zeta(k)} e^{-\pi\lambda} \mu f_{\alpha,-\lambda}}{e^{\pi\lambda} \mu f_{\alpha,-\lambda}^* + e^{2i\zeta(k)} f_{\alpha,\lambda}^*} \right] e^{-2i\alpha \ln(2kr)} \quad (23)$$

where $f_{\alpha,\lambda} = \frac{\Gamma(1+2i\lambda)}{\Gamma(1+i\lambda-i\alpha)}$. From (23) we obtain the scattering phase as

$$\delta_\nu(k) = \arg[e^{-i\zeta(k)} + b e^{i\zeta(k)}] - \alpha \ln(2kr) + \arg(f_{\alpha,\lambda}) \quad (24)$$

where $b = e^{-\pi\lambda} \mu \frac{f_{\alpha,-\lambda}}{f_{\alpha,\lambda}}$. In Fig. (3a) we plot (24) ignoring the Coulomb tail term $-\alpha \ln(2kr)$. For $\nu = 0.3$, the value of $\alpha = 1.8$ is deeper in the supercritical region than it is for $\nu = 1.5$. When the coupling α is deeper in the supercritical region, the phase shift has more number of kinks, which indicate the bound states. The plot also shows that the phase shift depends on the topology through its dependence on n via ν .

As mentioned before, in gapless graphene we do not expect bound states due to Klein tunneling. However, in the supercritical regime, the system admits quasi-bound states whose spectrum is obtained from the zeroes of the S matrix in (23). The quasi-bound state energies are given by

$$k_p = \frac{1}{2a_0} \exp \left[-\frac{p\pi}{\lambda} + i \left(\frac{1}{2\alpha} - \frac{\pi}{2} \right) \right], \quad (25)$$

where p is a positive integer.

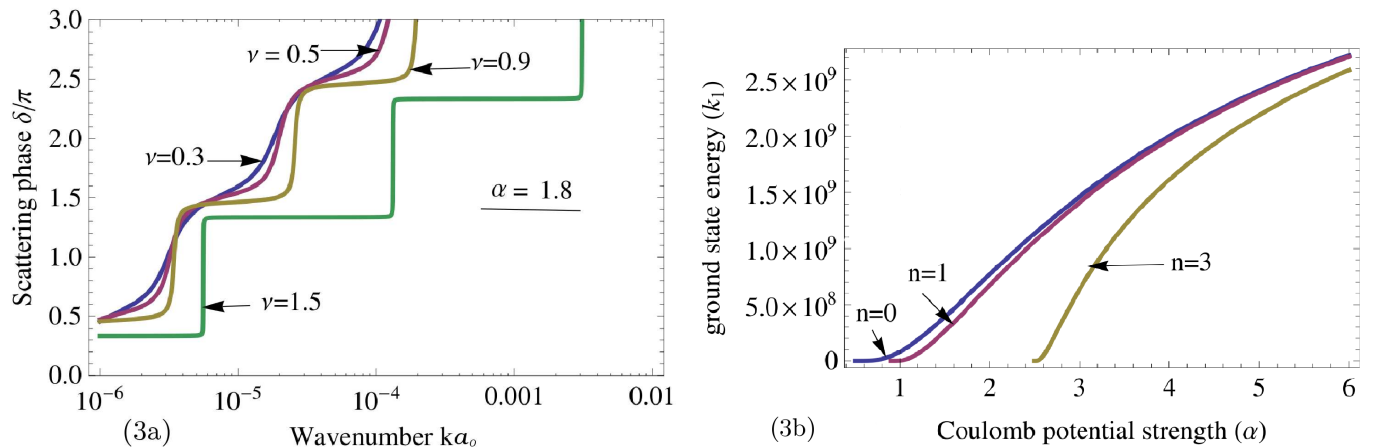


FIG. 3: (3a) shows the dependence of scattering phase shift δ on wavenumber ka_0 for $\nu = 0.3, 0.5, 0.9, 1.5$ and $\alpha = 1.8$, ignoring the Coulomb tail term $-\alpha \ln(2kr)$. As the value of ν increases, the kinks in the phase shift become sharper, which indicates the dependence of the phase shift on the angle of the graphene cone. (3b) shows dependence of ground state energy on the Coulomb potential strength for different angles of the graphene cone. We have considered $\nu = \frac{j+\frac{3}{8}}{1-\frac{3}{8}}$ and $j = \frac{1}{2}$.

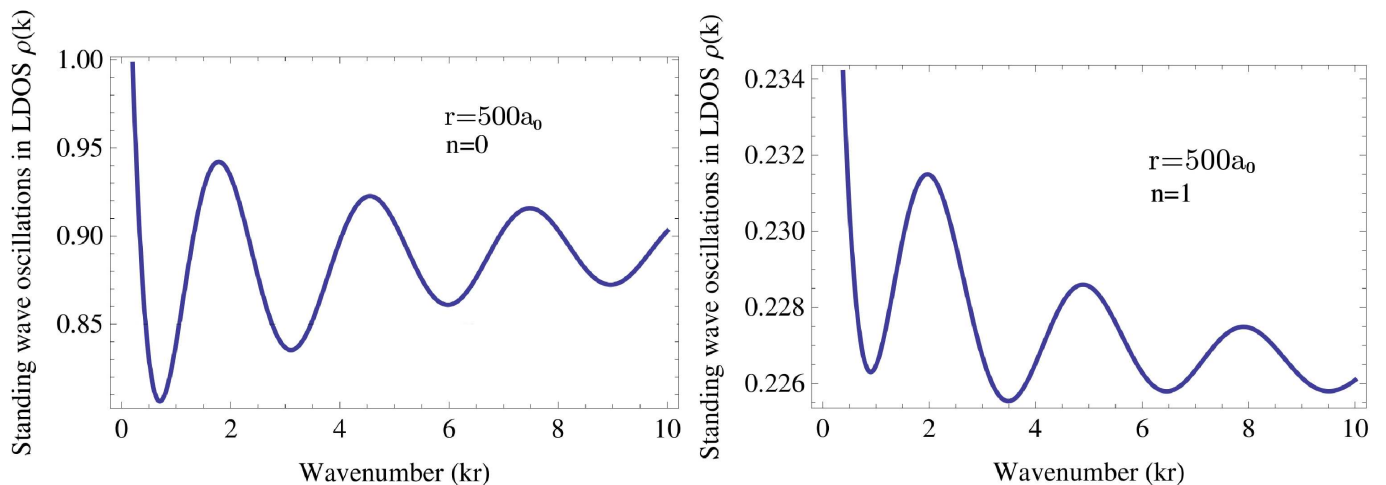


FIG. 4: Energy dependence of LDOS in presence of a Coulomb potential for different values of n and a particular value of r and with $j = \frac{1}{2}$ and $\alpha = 0.6$. This is in the supercritical region for both $n = 0$ and 1.

Another interesting observable in this context is the LDOS. In Fig.(4) we have plotted the standing wave oscillations in LDOS $\rho(k, r)$ using

$$\rho(k, r) = \frac{4}{\pi \hbar v_F} \sum_j |\Psi^{(j)}(k, r)|^2, \quad (26)$$

where $\Psi^{(j)}(k, r)$ is the radial part of the spinor given in Eq.(14), for a given angular momentum channel j . The maxima and minima of the oscillations occur at half-integral and integral multiple of π respectively. The normalization constant of the wave function depends on the value of n which decreases with increasing n . Therefore, though the nature of standing wave oscillation is similar for $n = 0$ and 1, the amplitudes of the corresponding LDOS decreases with the increase of n .

It is known that in the planar case, under the RG flow, a supercritical charge is driven to its critical value [16]. While the full discussion of the RG flow requires a more detailed analysis, we can obtain some of its qualitative features from the quasi-bound state energies. To see this consider the real part of k_p in (25) which gives the energy. This part diverges as the cutoff $a_0 \rightarrow 0$. In order to study the RG flow, we now promote the coupling constant α as

a function of a_0 and demand that as $a_0 \rightarrow 0$, the energy for any fixed level p (say $p = 1$) remains independent of the cutoff [26, 27]. In the leading order, where α is only slightly above the critical coupling, this prescription gives the β -function as

$$\beta(\lambda) \sim -\lambda^2 + .. \quad (27)$$

Thus we have an ultraviolet stable fixed point at $\lambda = 0$ or at $\alpha = \nu$. Hence, for any given value of n and j , the coupling α in the supercritical regime is driven to its critical value.

We end this Section with a comment for the case $\nu = 0$, which occurs for $n = 2$ and $j = \pm\frac{1}{2}$. For $\nu = 0$, the first order Dirac equations (17) and (18) completely decouple and the functions u and v become independent of each other. In this case, the critical coupling α_c also vanishes. This means that any external charge, no matter how small, would lead to the supercritical regime.

CONCLUSION

In this paper we use the fact that system of a graphene cone with an external Coulomb charge at its apex can be equivalently described by the combination of the Coulomb charge and a suitable magnetic flux tube passing through the apex. The above analysis has been done in the supercritical regime, where the external Coulomb charge exceeds a certain critical value.

The quantities of physical interest in this system include the scattering phase shifts, the LDOS and the quasi-bound state energies. We have shown that all these physical quantities depend explicitly on the number of sectors removed from a planar graphene to form the cone. The existence of the quasi-bound states indicates the possibility of the localization of the wavefunctions in the presence of a supercritical charge. Our analysis shows that the nature and extent of the localization depends on the spatial topology of the graphene sample.

Finally, we have given qualitative arguments which shows that under the RG flow and for $\nu \neq 0$, the supercritical charge in the graphene cone tends to its critical value. If this argument can be extended for $\nu = 0$, for which the critical charge vanishes, that would lead to complete shielding of the external charge. This issue and the related electronic properties are currently under investigation.

* Electronic address: baishali.chakraborty@saha.ac.in

† Electronic address: kumars.gupta@saha.ac.in

‡ Electronic address: siddhartha.sen@tcd.ie

- [1] K. S. Novoselov, A. K. Geim, S. V. Morozov, D. Jiang, M. I. Katsnelson, I. V. Grigorieva and A. A. Firsov, *Science* **306**, 666 (2004).
- [2] K. S. Novoselov, A. K. Geim, S. V. Morozov, D. Jiang, M. I. Katsnelson, I. V. Grigorieva, S. V. Dubonos and A. A. Firsov, *Nature* **438**, 197 (2005).
- [3] Y. Zhang, Y.-W. Tan, H. L. Stormer and P. Kim, *Nature* **438**, 201 (2005).
- [4] P.E. Lammert, V.H. Crespi, *Phys. Rev. Lett.* **85**, 5190 (2000).
- [5] P.E. Lammert, V.H. Crespi, *Phys. B* **69**, 035406 (2004).
- [6] D. V. Kolesnikov and V. A. Osipov, *Eur. Phys. J. B* **49**, 465 (2006).
- [7] A.Cortijo, M.A.H.Vozmediano, *Nucl. Phys. B* **763**, 293 (2007).
- [8] C.Furtado, F.Moraes, A.M. de M. Carvalho, *Phys. Lett. A* **372**, 5368 (2008).
- [9] A. Roy and M. Stone, *J. Phys. A* **43**, 015203 (2010).
- [10] Wallace, P. R. The band theory of graphite. *Phys. Rev.* 71, 622634 (1947).
- [11] A. K. Geim and K.S. Novoselov, *Nature Materials* 6, 183-191 (2007).
- [12] A.H.Castro Neto, F.Guinea, N.M.R. Peres, K.S. Novoselov and A.K.Geim, *Rev. Mod. Phys.* 81, 109 (2009).
- [13] D. P. DiVincenzo and E. J. Mele, *Phys. rev. B* **29**, 1685 (1984).
- [14] G. W. Semenoff, *Phys. Rev. Lett.* **53**, 2449 (1984).
- [15] V. M. Pereira, J. Nilsson and A. H. Castro Neto, *Phys. Rev. Lett.* **99**, 166802 (2007).
- [16] A. V. Shytov, M. I. Katsnelson and L. S. Levitov, *Phys. Rev. Lett.* **99**, 236801 (2007).
- [17] A. V. Shytov, M. I. Katsnelson and L. S. Levitov, *Phys. Rev. Lett.* **99**, 246802 (2007).
- [18] A. Shytov, M. Rudner, N. Gu, M. Katsnelson and L. levitov, *Solid State Comm.* **149**, 1087 (2009).
- [19] Kumar S. Gupta and Siddhartha Sen, *Mod. Phys. Lett. A* **24**, 99 (2009).
- [20] M. I. Katsnelson, K. S. Novoselov and A. K. Geim, *Nature Physics* **2**, 620 (2006).
- [21] N. Dombey, A. Calogeracos, *Physics Reports* 315 (1999).
- [22] O. Klein, *Z. Phys.* 53 (1929) 157.

- [23] M.I.Katsnelson and K.S. Novoselov, Solid State Communications, Volume 143, Issues 1-2, July 2007, Pages 3-13.
- [24] W. Greiner, B. Muller, and J. Rafelski, Quantum Electrodynamics of Strong Fields (Springer-Verlag, Berlin, 1985).
- [25] J. Reinhardt and W. Greiner, Rep. Prog. Phys. **40**, 219 (1977).
- [26] K. S. Gupta and S. G. Rajeev, Phys. Rev. **D 48**, 5940 (1993).
- [27] Kumar S. Gupta and Siddhartha Sen, Phys. rev. **B 78**, 205429 (2008).